RASIP1 REGULATES VASCULAR TUBULOGENESIS

APPROVED BY SUPERVISORY COMMITTEE

Ondine Cleaver, Ph.D.

Thomas Carroll, Ph.D. (Chair)

Melanie Cobb, Ph.D.

Eric Olson, Ph.D.

To

My family

ACKNOWLEDGEMENT

I am extremely grateful to Dr. Ondine Cleaver, who has been the greatest mentor and best friend to me. I feel super lucky to be able to join her laboratory. It was in this most friendly and encouraging family-like environment that she has created for everyone of us I realized just how much I enjoy the challenges and rewards of scientific research. Being a Cleaver lab member has been one of the most cherished memories of my life.

My deepest gratitude also goes to my committee members, Drs. Thomas Carroll (Chair), Melanie Cobb and Eric Olson. Their great insights, passions in science, invaluable advice and unconditional support have always kept me on the right track and driven me to pursue higher goals. I also want to thank them for their efforts in creating the best graduate school and the best research department for all of us. They are my role models in my scientific career.

I want to thank Dr. Michael Haberland. The tremendous amount of ideas and amazing hands-on experiences he shared with me in molecular biology will be a life-long benefit.

I'd like to thank all the Cleaver lab, current and past members, particularly Diana Chong, Alethia Villasenor, Brian Fairbanks and Stephen Fu for their great help in developing ideas and carrying out experiments. Also thanks to

all other lab mates Stryder Meadows, Peter Fletcher, Yeon Koo, Lelani Marty, David Barry for their support and friendship.

I also want to thank all the technical and administrative staffs of the graduate school, the Genetics & Development program, and the Molecular Biology Department for their daily support.

Last but not least, I want to give my greatest thanks to my wife Qiuping Chen ( ), my parents Xin Zheng ( ) and Bailing Xu ( ), my sister Duo Xu ( ) and all my family for their endless love. They are pillars of my life.

RASIPA REGULATES VASCULAR TUBULOGENESIS

by

Ke Xu ( )

DISSERTATION

Presented to the Faculty of the Graduate School of Biomedical Sciences

The University of Texas Southwestern Medical Center at Dallas

In Partial Fulfillment of the Requirements

For the Degree of

DOCTOR OF PHILOSOPHY

The University of Texas Southwestern Medical Center at Dallas

Dallas, Texas

May, 2011

RASIPA REGULATES VASCULAR TUBULOGENESIS

Ke Xu, Ph.D.

The University of Texas Southwestern Medical Center at Dallas, 2011

Mentor: Ondine Cleaver, Ph.D.

Cardiovascular function depends on patent blood vessel formation by endothelial cells (ECs). However very little is known about the mechanisms underlying vascular tubulogenesis. This study identifies Rasip1 as a unique, endothelial-specific regulator of Rho GTPase signaling, which is essential for endothelial lumen morphogenesis. We found that *Rasip1* is strongly expressed in vascular endothelial cells throughout development across species. Similar to the well-characterized vascular markers *VEGFR2* and *PECAM, Rasip1* is specifically expressed in angioblasts prior to vessel formation, in the initial embryonic vascular plexus, in the growing blood vessels during angiogenesis and in the endothelium of mature blood vessels into the postnatal period. *Rasip1* expression is undetectable in *VEGFR2* null embryos, which lack endothelial cells, suggesting that *Rasip1* is endothelial-specific.

Ablation of *Rasip1* both *in vitro* and *in vivo* strongly affects vascular integrity. Specifically, siRNA-mediated reduction of *Rasip1* severely impairs angiogenesis in endothelial cell cultures, and morpholino knockdown experiments demonstrate that *Rasip1* is required for embryonic vessel formation in frog embryos. Mice lacking *Rasip1* fail to form patent lumens in all blood vessels, including the early endocardial tube. *Rasipl* null angioblasts fail to properly localize the polarity determinant Par3 and display defective cell polarity, resulting in mislocalized junctional complexes and loss of adhesion to extracellular matrix (ECM). Depletion of either *Rasip1* or its binding partner RhoGAP *Arhgap29* in cultured ECs blocks *in vitro* lumen formation, fundamentally alters the cytoskeleton and reduces integrin-dependent adhesion to ECM. These defects result from increased RhoA/ROCK/myosin II activity and blockade of Cdc42 and Rac1 signaling. Together, our work identify *Rasip1* as a novel endothelial factor that plays an essential role in vascular tubulogenesis.

TABLE OF CONTENTS

LIST OF PUBLICATIONS

1) **Ke Xu**, Anastasia Sacharidou, Stephen Fu, Diana C. Chong, Brian Skaug, Zhijian J. Chen, George E. Davis and Ondine Cleaver. *Blood vessel tubulogenesis requires Rasip1 regulation of GTPase signaling.* ***Development Cell***. 2011; 20(4): 526-539.

2) Jian Xie, Tao Wu, **Ke Xu**, Ivan K. Huang, Ondine Cleaver, and Chou-Long Huang. *Endothelial-Specific Expression of WNK1 Kinase Is Essential for Angiogenesis and Heart Development in Mice*. ***The American Journal of Pathology***. 2009; 175(3):1315-27.

3) **Ke Xu**, Diana Chong, Scott Rankin, Aaron Zorn and Ondine Cleaver. *Rasip1 is required for endothelial cell motility, angiogenesis and vessel formation.* ***Developmental Biology***. 2009; 329(2):269-79.

4) Ondine Cleaver, Dan Quiat, **Ke Xu**, Alethia Villasenor. *Morphogenesis of blood vessels during mouse vasculogenesis (Abstract)*. ***Developmental Biology***. 2007; 306(1):445.

5) YuRui Zhao, Quan Zheng, Kenneth Dakin, **Ke Xu**, Manuel L. Martinez, and Wen-hong Li. *New Caged Coumarin Fluorophores with Extraordinary Uncaging Cross Sections Suitable for Biological Imaging Applications.* ***J. Am. Chem. Soc.*** 2004; 126(14) pp4653 ï4663 (Article).

6) Ying-Jie Wang, Wen-hong Li, Jing Wang, **Ke Xu**, Ping Dong, Xiang Luo, and Helen L. Yin. *Critical role of PIP5KIg87 in $InsP_3$-mediated Ca^{2+} signaling.* ***Journal of Cell Biology***. 2004; 167(6) 1005-1010.

LIST OF FIGURES

LIST OF TABLES

LIST OF ABBREVIATIONS

AJ	Adhesion Junction
BMP	Bone Morphogenetic Protein
BSA	Bovine Serum Albumin
cDNA	Complementary DNA
DIG	Digoxigenin
DNA	Deoxyribonucleic Acid
EC	Endothelial Cell
EGFP	Enhanced GFP
EST	Expressed Sequence Tag
FA	Focal Adhesion
FB	Fibrillar Adhesion
FBS	Fetal Bovine Serum
Flk1	Fetal Liver kinase 1
FN	Fibronectin
FX	Focal Complex
GAP	GTPase Activating Protein
GDP	Guanosine-5'-diphosphate

GEF	Guanine Exchange Factor
GFP	Green Fluorescent Protein
GTP	Guanosine Triphosphate
HPRT	Hypoxanthine-guanine Phosphoribosyltransferase
ISV	Intersomitic/Intersegmental Vessel
KDR	Kinase insert Domain Receptor
MO	Morpholino
PBS	Phosphate Buffered Saline
PCR	Polymerase Chain Reaction
PECAM	Platelet Endothelial Cell Adhesion Molecule
PFA	paraformaldehyde
RT-PCR	Reverse Transcriptase-PCR
siRNA	small interfering RNA
T G F ß	Transforming Growth Factor beta
Tie2	Tyrosine kinase with immunoglobulin-like and EGF-like domain 2
TJ	Tight Junction
VEGF	Vascular Endothelial Growth Factor

VEGFR2	VEGF Receptor 2
TEM	Transmission Electron Microscopy

CHAPTER I

Introduction

The cardiovascular system is the first functional organ system to form in the developing embryos across all vertebrate species, providing tissues with nutrient and gas exchange required for life. Defects in the structure and/or function of the cardiovascular system lead to early embryonic lethality. The vasculature emerges from aggregation of *angioblasts*. Angioblasts are endothelial precursors that arise from mesodermal cells that differentiate either within blood islands, structures composed of hematopoietic cells (blood cell precursors) surrounded by a mantle of angioblasts, or within embryonic tissues as scattered cells in both extraembryonic and embryonic tissues. Vessels subsequently form via v*asculogenesis*, or the coalescence *in situ* of individual solid primitive vascular ócordsô (Drake and Fleming, 2000; Risau and Flamme, 1995). These lumenless, linear aggregates then transform into tubes to carry blood. The first vessels consist of a relatively simple and homogeneous endothelial cell EC network of vessels, often termed a óplexusô. Subsequently, the complexity of which then

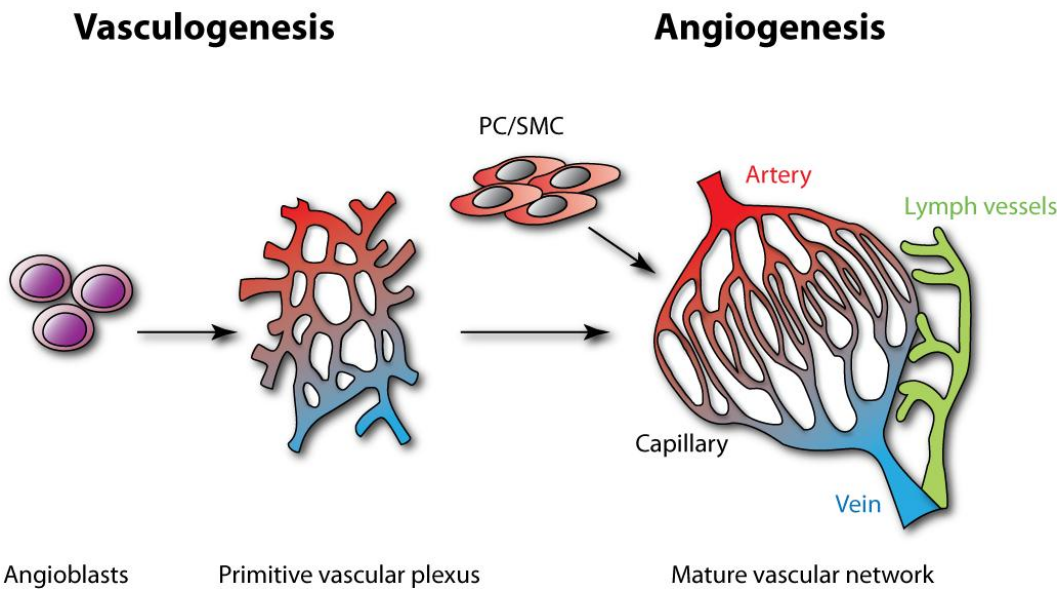

Figure 1.1. Development of the vascular systems (adapted and redrawn from (Carmeliet, 2005)). During vasculogenesis, angioblast derived ECs form a primitive vascular plexus de novo. This initial network is then undergo a process called angiogenesis including the remodeling, sprouting and pericyte/smooth muscle cells (PC/SMC) stabilizing of the vessels to form a mature vasculature containing a complex network of large and small vessels. Lymphangiogenesis initiates from veins.

as new vessels sprout from pre-existing vessels via sprouting *angiogenesis* (Carmeliet, 2000; Risau, 1997). Sprouting extends existing lumens and rearrange the initially simple, net-like, primary tubular network, via remodeling *angiogenesis*, into a complex hierarchical system, which includes specialized ECs, such as arteries and veins. As these vessels mature and stabilize, they become ensheathed by smooth muscle cells and pericytes. However, they continue to grow coordinately with organs and tissues, providing the tissues they perfuse with the nutrients and oxygen required for viability (**Figure 1.1**).

Vasculogenic tubulogenesis: cord-to-tube transition

Formation of a cohesive seamless and contiguous network of blood vessels to carry blood is essential for proper cardiovascular function. However, while a growing understanding is emerging regarding the specification, patterning and sprouting of blood vessels, the mechanisms underlying the cellular morphogenesis and molecular pathways that direct vascular tubulogenesis are only beginning to be unraveled. Tubulogenesis is a fundamental process that is essential for the development of many tubular organs. During vasculogenesis, the angioblast-formed linear vascular cords undergo a morphogenic change during which the angioblasts transition from a cuboidal to a flattened shape to encircle a

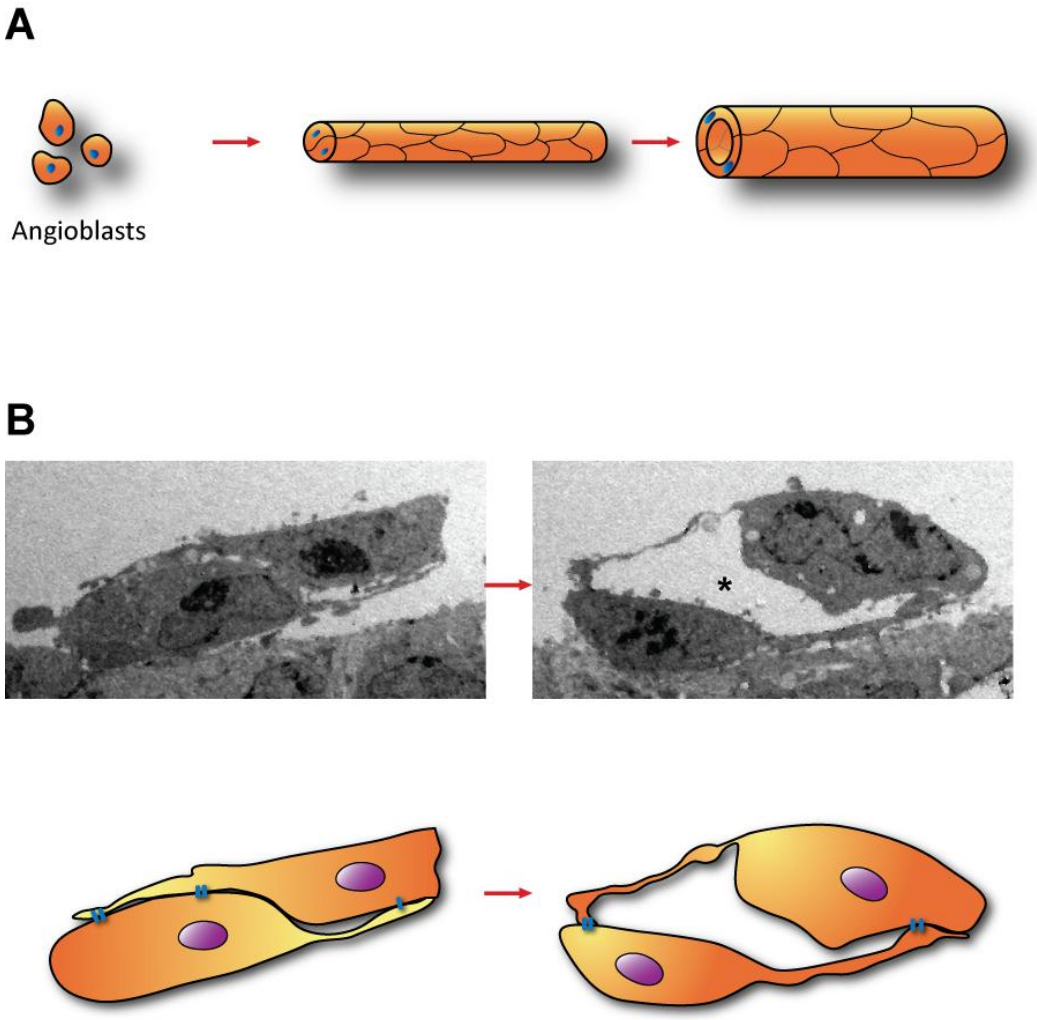

Figure 1.2. Vasculogenic tubulogenesis: cord-to-tube transition. (**A**) Morphogenic changes of angioblasts from single cells to linear cords and patent tubes. (**B**) TEM images and cartoons showing two angioblasts before and after cord-to-tube transition. Junctional molecules are represented as blue bars. asterisk in TEM region: vascular lumen between two ECs.

central lumen (**Figure 1.2A**). This step is fundamental to establishing a functional circulatory system. Dramatic cellular changes take place during this process, including the re-localization/distribution of junctional molecules to cell periphery allowing the opening of the initial 3D lumen (**Figure 1.2B**).

Angiogenic tubulogenesis: lumen extension

Similar to de novo lumen and tube formation in initial embryonic vessels, lumens must also form in new angiogenic sprouts. However, the mechanisms are likely to differ to some extent, as initial vessels start as solid cords with no connections to existing lumens, while angiogenic vessels grow from pre-existing tubes, with pre-existing lumens (**Figure 1.3**). Much work has recently focused on sprout formation and the role of VEGF and Notch signaling during this process. The distal growing end of angiogenic vessels consists of endothelial tip cells which extend long filopodia and migrate in a manner similar to axonal growth cones, sensing their microenvironment. The proximal end of these vessels, by contrast, consists of stalk cells that form a trailing cord or quickly become lumenized (Gerhardt et al., 2003; Holderfield and Hughes, 2008). The process that controls tip cell growth is dependent on a remarkable interplay of selective Notch ligand activation, as well as the establishment of well-controlled VEGF gradients (Chappell et al., 2009). To date, however, relatively little

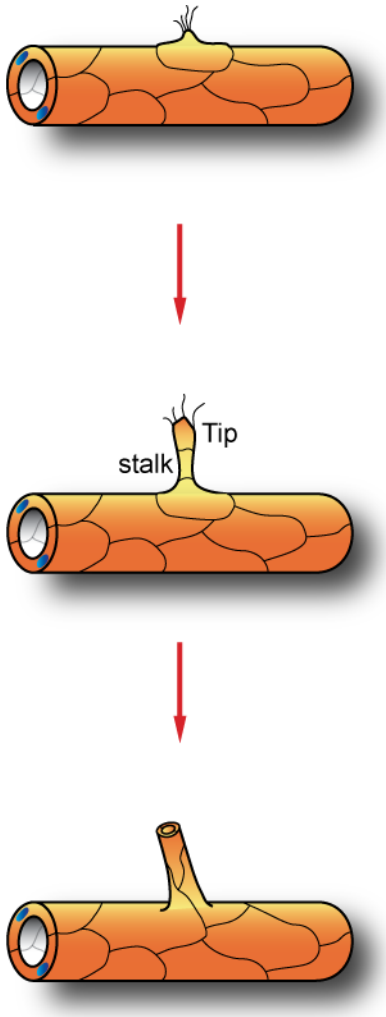

Figure 1.3. Angiogenic tubulogenesis: lumen extension.

attention has been focused on the timing, mechanics or molecular regulation of lumen formation in stalk cells. Comparing and contrasting lumen formation in different types of vessels will reveal whether similar mechanisms apply to all vessels or whether locally distinct modes of lumen formation will reflect inherent heterogeneity of vessels.

Cellular mechanisms of vascular tubulogenesis

As a tubular organ, the endothelial vasculature shares a lot of common features with epithelial tubes found in a number of other organs. A considerable amount of work has been carried out to elucidate epithelial tubulogenesis during the past several decades. Epithelial tubes are present in many organs including lung, kidney, salivary glands and pancreas. These tubes are generally composed of a sheath of cuboidal or columnar epithelial cells, with defined apical membranes facing a central lumen, their lateral edges interfacing with each other closely, and their basal membranes making up the tube periphery (**Figure 1.4A**). Similarly, ECs of functional vessels consist of a luminal (apical) membrane facing the flowing blood and an abluminal (basal) membrane in contact with the basement membrane. The principal difference between epithelial and endothelial tubes is that the junctional contacts (lateral membranes) between ECs consist of a much smaller contact area (**Figure 1.4B**).

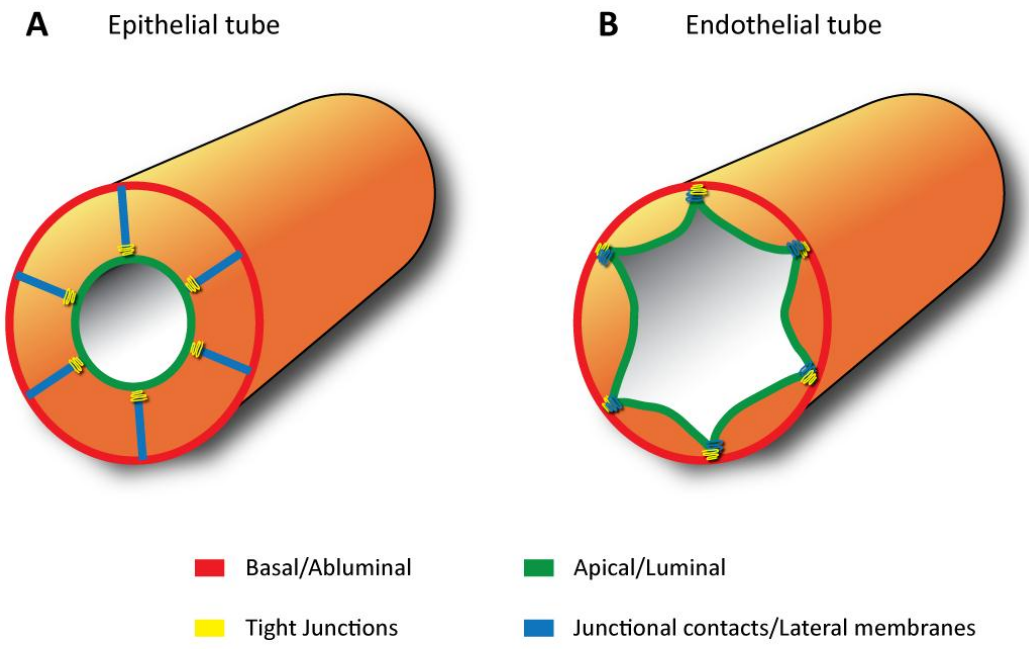

Figure 1.4. Junctional contacts in epithelial and endothelial tubes. Compared to lumen forming epithelial cells, endothelial cells display much smaller junctional contacts/Lateral membranes.

Nonetheless, a number of analogies between the two tissue types can be made. Depending on the types of organs and microenvironments, most epithelial tubulogenesis processes fall into one or a combination of several of the following categories: wrapping (i.e. vertebrate primary neurulation), budding (i.e. lung), cell hollowing (i.e. Drosophila trachea), cord hollowing (i.e. zebrafish gut), cavitation (i.e. salivary gland), and cell division and intercalation (i.e. zebrafish neural tube) (Andrew and Ewald, 2010; Lubarsky and Krasnow, 2003). Among these mechanisms, at least three have been implicated in endothelial lumen formation: budding, cell hollowing and cord hollowing (Iruela-Arispe and Davis, 2009).

(1) Budding

By definition, budding consists of formation and extension of a tube via growth from a pre-existing tube. During lung development, the pulmonary epithelium repeatedly buds and extends finger-like projections, until it becomes a continuous, highly branched, tubular tree. During blood vessel formation, sprouting angiogenesis is essentially synonymous with budding (**Figure 1.3**).ECs along the wall of a blood vessel become locally activated, degrade the surrounding basement membrane, cells migrate out, with tip cells at the leading front of the growing vessel invading surrounding tissue. As angiogenic sprouting gives rise to patent vessels, it can thereby be considered one mechanism for lumen

formation. Howeve, what processes specifically drive stalk cells to organize, extend and maintain the parental lumen remain unclear.

(2) Cell hollowing: vacuole fusion

In contrast to budding where new lumens extend directly from pre-existing lumens, cell hollowing represents a different cellular mechanism whereby new lumens emerge intracellularly. In this case, lumens initiate as multiple small vesicles or larger vacuoles, that fuse to produce a central lumen, which in turn becomes connected with similar lumens in adjacent cells (**Figure 1.5A**). This type of lumen formation has been observed in Drosophila terminal tracheal cells (Guillemin et al., 1996; Levi et al., 2006), as well as in ECs. Indeed, until recently vascular lumen formation had primarily been studied in vitro, and a large body of work using live imaging of ECs in 3D matrices has demonstrated that intraendothelial lumen formation occurs by cell hollowing via vacuole fusion (Davis et al., 2000; Iruela-Arispe and Davis, 2009; Sacharidou et al., 2010). Vacuole fusion has also been observed *in vivo*, during formation of intersegmental vessels in zebrafish (Kamei et al., 2006). Together, these observations suggested that cell hollowing was an important mechanism in both endothelial and non-endothelial tubulogenesis.

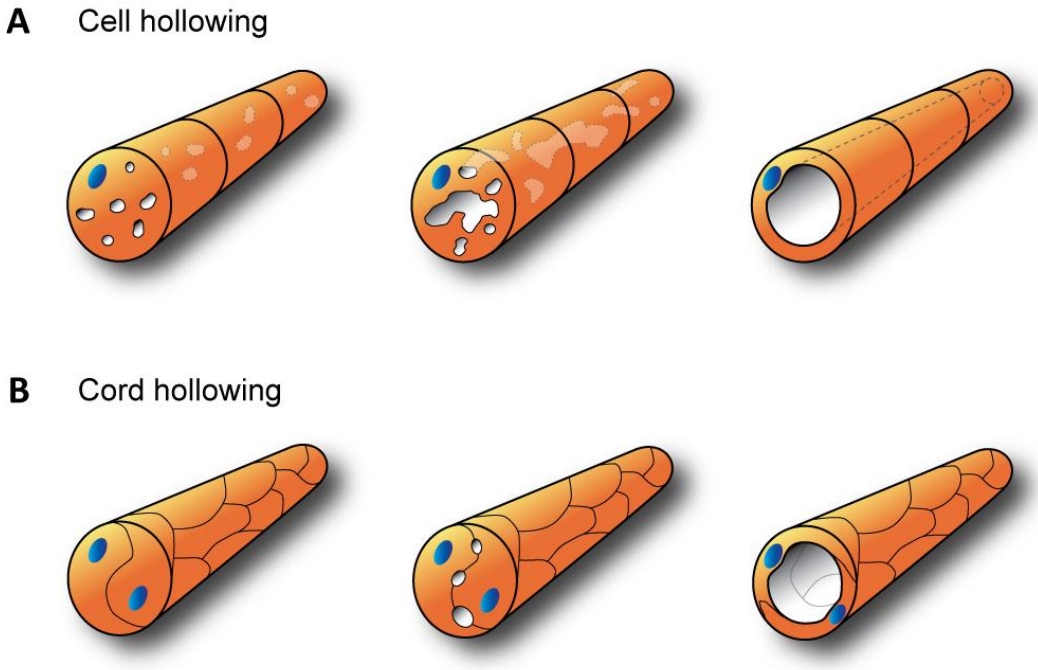

Figure 1.5. Vascular tubulogenesis: Cell hollowing vs. Cord hollowing.

(3) Cord hollowing: vacuole fusion and cell rearrangement

A third type of mechanism by which some lumens form is termed cord hollowing. In this process, lumenal spaces generated extracellularly between ECs, even as they remain joined peripherally (**Figure 1.5B**). Expansion of apical membranes to create an intervening extracellular space can be achieved either by addition of new lumenal membrane, or by removal or clearance of junctions from the cord center. The result of either process is to build up the net surface area of the lumenal membrane.

Addition of new lumenal membrane during lumen formation has been shown in some cases to occur via directed exocytosis of vesicles, which fuse with and expand the lumen at the cord center. This type of vectorial vacuole fusion has been observed in cultured MDCK epithelial cells (Lipschutz et al., 2000; Lubarsky and Krasnow, 2003; Vega-Salas et al., 1988). It has also been shown in endothelial cells and suggested to be dependent on Rab7-directed centripetal transport of vacuoles (Zovein et al., 2010). Interestingly, both cell polarity and proper control of cell adhesion appear to provide a critical framework for this process, as loss of β1 integrin disrupts Par3 lo

Vascular tubulogenesis: mechanistic heterogeneity

Tubulogenesis has fascinated developmental and cell biologists for decades and recent efforts have been directed towards understanding it in vertebrate blood vessels (Hogan and Kolodziej, 2002; Stuart et al., 1995; Zeeb et al., 2010). As the number of studies has increased, our understanding of the underlying mechanisms has evolved. Until recently, cell hollowing was considered a common, if not predominant, mode of *de novo* endothelial lumen formation. Clear live imaging of ECs cultured in 3D matrices provided strong support for vacuole-based lumen formation (Davis et al., 2000). Cells were shown to generate intracellular vacuoles that would align at the cell center and fuse with each other to create lumens.

Similarly, vacuole fusion has been observed in the growing vessels of vertebrate embryos (Blum et al., 2008; Kamei et al., 2006; Liu et al., 2011; Wang et al., 2010) (**Figure 1.6A**). Live imaging of growing zebrafish intersegmental vessels (ISVs) identified fusing vacuoles during lumen formation (Kamei et al., 2006). This study examined at high resolution the development of ISVs, which were thought to assemble stereotypically with three ECs in a head-to-tail cord along myotomal boundaries (Isogai et al., 2003). Two photon live cell imaging identified vacuoles during angiogenic sprouting and suggested intra-cellular fusion of endothelial vacuoles at the center of ISV ECs suggesting cell hollowing.

Also required for expansion of extracellular space and tubulogenesis is the de-adhesion and/or redistribution of junctional molecules at the cord center. In this case, cells within a cord create a lumen by de-adhering from each other locally at the luminal membrane, but remaining tethered at the lumen periphery. This differential adhesion thereby alters EC shape and rearranges ECs relative to each other. Alternately, ECs might also redistribute existing junctions to the periphery, away from the lumen. Such junctional redistribution has been observed in the gut epithelium of zebrafish (Horne-Badovinac et al., 2001) and more recently during vasculogenesis in mouse (Xu et al., 2011) (**Figure 1.6C**).

To date no definitive experimental evidence has clearly distinguished lumenal membrane expansion, versus either de-adhesion or clearance of junctions, however it is very possible that a number of cellular phenomena occur coordinately during lumen formation. Indeed, both directed vacuolar transport and junctional redistribution have been observed to occur concurrently in the arterioles of late gestation mouse embryos (Zovein et al., 2010). These vessels arise first as cords of cuboidal ECs, which then open a central lumen following redistribution of junctional molecules to the cord periphery (away from the center) and Rab7-directed vesicle transport to the lumenal membrane (**Figure 1.6B**). It will be of great interest to assess whether both mechanisms apply more globally to forming vessels.

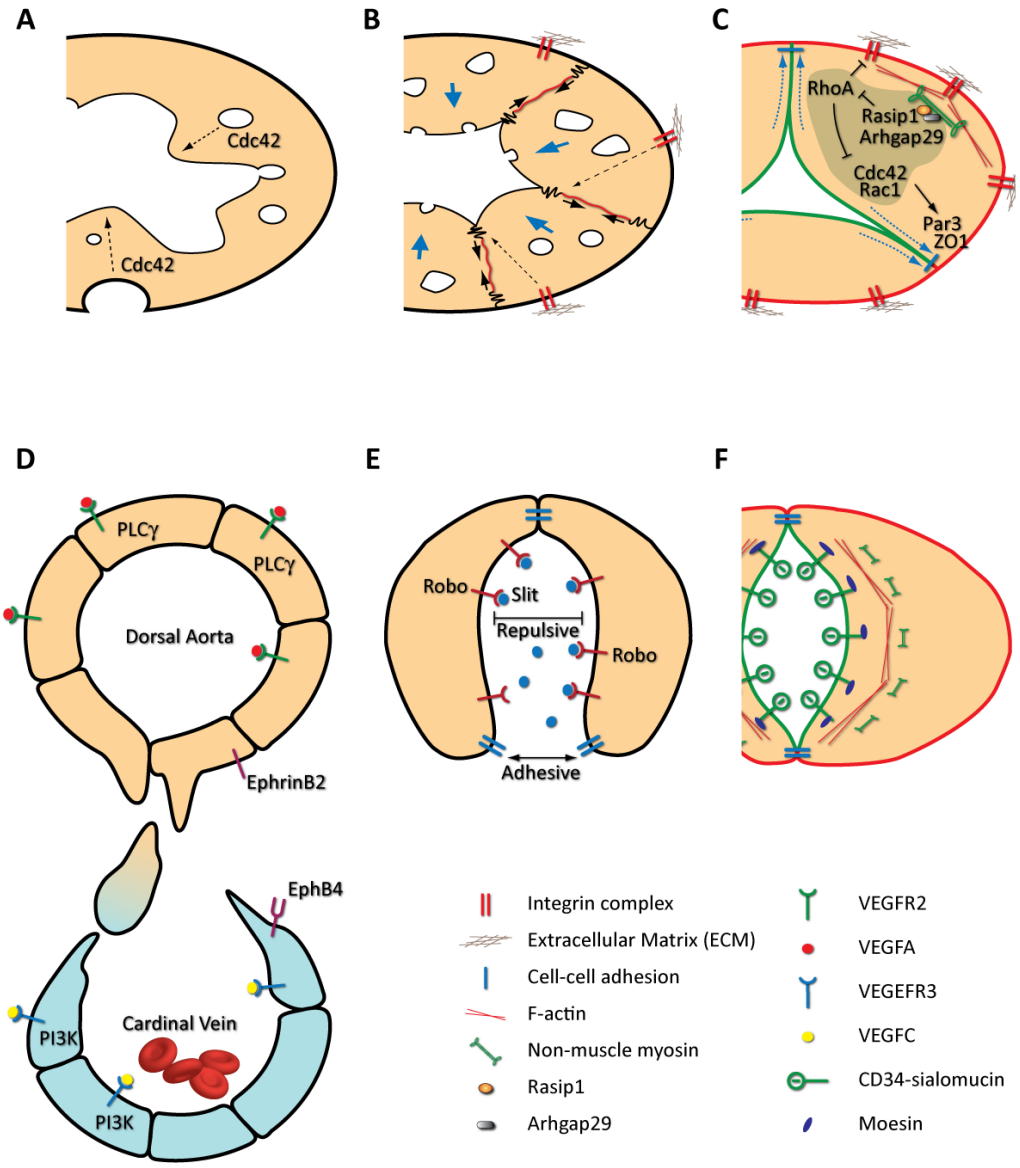

Figure 1.6. Vascular tubulogenesis: mechanistic heterogeneity. (**A**) Vacuole fusion. (**B**) integrin induced cell polarity formation. (**C**) Rasip1-Rho regulated integrin-acto-myosin activity. (**D**) Zebrafish cardinal vein formation. (**E**) Repulsive signal mediated Drosophila heart tube formation. (**F**) Acto-myosin and negative charges mediated vascular slit initiation.

The existence of a variety of mechanisms is highly likely, however, given the endothelial heterogeneity that is known to exists in different vascular beds. One example involves lumen formation during initial arteriovenous segregation in zebrafish (Herbert et al., 2009) (**Figure 1.6D**). High-resolution imaging of zebrafish vascular morphogenesis showed that the primary axial dorsal aorta (artery) arises first by vasculogenic aggregation of angioblasts. Secondarily, the caudal vein develops via selective ventral sprouting and migration of angioblasts from the dorsal aorta, a process they show to be regulated by EphrinB2-EphB4 signaling. Interestingly, the caudal lumen forms via angioblasts aggregating into a partially open vessel, which then rapid accumulated at the interface of the two ve vein, a cardiovasculature with functional circulation is then rapidly established. The cellular mechanisms underlying this open vessel formation examined, but suggest the probability of a variety of mechanisms underlying tubulogenesis.

Yet another divergent mechanism for ñbl reported during Drosophila heart morphogenesis (Medioni et al., 2008; Santiago-Martinez et al., 2008) (**Figure 1.6E**). In flies, the heart represents an open-ended and contractile endolymph vessel of sor distinct internal lumen. In these studies, formation of the cardiovascular lumen by two parallel rows of myoendothelial cells is shown to be modulated by membrane

repulsion. Slit-Robo signaling downregulates E-cadherin at the lumenal cell-surface and prevents fusion between apposed cells. Instead, the two cells form junctions only at their dorsal- and then ventral-most regions, resulting in the formation of an internal central lumen, enclosed by two rows of cells. Even more interestingly, distinct from typical epithelial tubulogenesis processes, the fly heart lumen formed by this mechanism is created by the basal rather than apical cell surfaces, suggesting that fundamental differences can occur between different types of epithelial and endothelial tube forming cells with respect to cell polarity features.

A similar lumenal repulsion mechanism has also been suggested during mouse dorsal aortae formation. Following cord hollowing, observations by Lammert and colleagues showed that accumulation of negatively charged sialomucins along apposed lumenal membranes results in the initial opening of slit-like spaces between ECs (Strilic et al., 2010; Strilic et al., 2009) (**Figure 1.6F**). Specifically, they show that sialic acids of lumenal glycoproteins create repulsive electrostatic fields that result in membranes moving away from each other at the cord center. Neutralizing these charges with injection of cationic protamine sulfates inhibits normal lumen formation.

Taken together, these many divergent examples of lumen formation mechanisms suggest that different vessels may form via a range of different

cellular mechanisms. It is not completely unexpected, as endothelium is known to display a high level of heterogeneity across different tissues (Aird, 2003). We propose that distinct or even yet to be di formation will likely be identified as vascular beds of different organs are more extensively examined and understood.

CHAPTER II

Materials and methods

Isolation of Rasip1 sequence

A pYX plasmid containing mouse *Rasip1* cDNA piece (1047 ï3170bp, spanning exons 4 through 7) was obtained from OpenBiosystems (BC072584). For making longer *in situ* probes, the full-length coding region (2886bp) of *Rasip1* was amplified from E8.5 mouse cDNA by RT-PCR, using primer set P1 (Table 2.1). *Xenopus tropicalis Rasip1* partial coding region sequence (1151bp, exon2-exon7) was cloned by RT-PCR using primer set P2. The amplified fragments were subcloned into pGEM-T-Easy Vector (Promega) by TA cloning.

Mouse strains

VEGFR2 null embryos were generated by mating Flk1(VEGFR2)-lacZ heterozygous males and females (kindly provided by Drs. Janet Rossant and Eli Keshet). Embryos were dissected manually in ice cold PBS. Embryos lacking blood vessels were identified visually, by the absence of yolk sac blood vessels,

and genotypes (of either embryos or adults) were confirmed by PCR, using primers to lacZ (Table 2.1), which yield a 630bp PCR fragment.

Embryos and Histology

CD1 mice embryos were collected from pregnant females (E7.5 through E15.5) after dissection in ice-cold PBS buffer and fixed in 4% PFA in PBS solution overnight at 4°C with gentle rocking. The amnion was removed during dissection for better probe penetration. Embryos were washed three times in PBS for 5 min, and dehydrated using a series of ethanol washes. Embryos were then stored in 75% ethanol at -20°C. Postnatal tissue was collected and fixed in a similar manner.

For wax sectioning of embryos following *in situ* hybridization, the embryos were fixed and dehydrated as described above. Embryos were rinsed twice in 100% ethanol for 5 min, twice in xylene at RT for 10 min, then a mixture of 1:1 paraplast : xylene at 60°C for 10 min, then a series of 100% paraplast at 60°C (McCormick Scientific). The embryos were then embedded and sectioned with a Biocut 2030 microtome. For examination, the sections were placed on glass slides, deparaffinized in xylene twice for 5 min each and mounted on SuperfrostPlus glass slides (Fisher) using Permount (Fisher).

DIG-labeled RNA probes

Probe synthesis was carried out at 37 overnight using 1µg linearized plasmid, 2.0µl DIG-RNA labeling mix (Roche), 2.0µl 10X transcription buffer (Roche), 1.5µl Placental ribonuclease inhibitor (Promega), 1.0µl T3/T7 RNA polymerase (Roche), RNase free water to a final volume of 20µl. DNA template was removed using 2µl RQ1 DNase I (Promega), at 37 °C for 15 min. The probes were then purified with Micro Bio-spin columns (Bio-RAD). 10x hybridization stock solution was prepared at a concentra 50% Formamide (Fisher), 5xSSC (pH 4.5), 50µg/ml Ribonucleic acid from Torula yeast, Type VI (Sigma), 1% SDS, 50µg/ml Heparin (Sigma). Stock solution is stored at ï20 °C.

Whole mount in situ hybridization

Whole mount *in situ* hybridization in mouse embryos was carried out using a protocol adapted from Wilkinson (Wilkinson, 1999). Briefly, embryos stored in 75% ethanol at ï20 ęC were rehydrated in ste PBST. Then, the embryos were treated with 10µg/ml proteinase K (time treated varied with age of tissue; 2min-30min), fixed in a 0.2% gluteraldehyde/4% PFA solution, and pre-hybridized at 65 °C for 1 hour. The samples were transferred into

hybridization mix, containing 1µg/ml Dig -labeled probes described above. The *in situ* hybridization post-hybridization washes and antibody incubation were carried out using a Biolane HTI automated incubation liquid handler (Holle & Huttner). Color development was carried out using BM purple solution (Roche). Frog *in situ* hybridization was carried out using a similar standard *in situ* hybridization protocol (Costa et al., 2003). Zebrafish *in situ*s were performed as previously described (Neumann et al., 2009).

In situ hybridization on sections

Paraffin sections (on glass slides) were washed 3x3min in PBS, followed by a 10min treatment with 15mg/ml proteinase K. Sections were then rinsed in PBS, fixed in 4% PFA for 5 min, and incubated for 10min in acetylation solution: mix of 2.66ml Triethanolamine, 350ml HCl, 750ml acetic anhydride and 200ml water. Prehybridization was carried out in plastic slide mailers (Fisher) containing hybridization buffer at RT for 1 hour. Slides were then transferred to a humidified chamber (humidified with 50% formamide/5xSSC) for probe hybridization (probe at 1mg/ml) with 100ml probe/slide (covered with glass coverslips) at 68℃ overnight.

Slides were washed post-hybridization in 2xSSC at 72℃ just long enough to allow coverslips to separate. Then slides were rinsed in 0.2xSSC at 72℃ and RT for 1x1min, respectively, then MBST buffer at RT (100mM Maleic acid, 150mM NaCl, pH7.5, 0.1% Tween20). Slides were incubated in blocking solution (2% blocking reagent (Roche) and 5% heat-inactivated sheep serum in MBST) for 1 hour at RT. Anti-DIG alkaline phosphatase conjugated antibody was applied on slides in a chamber humidified with MBST (250㎖ of 1/4000 anti-DIG antibody (Roche)), covered with parafilm and incubated at 4℃ overnight. Slides were washed for 3x30min in MBST after antibody incubation, and treated in NTMT (100mM NaCl, 100mM Tris, pH9.5, 50mM MgCl2, 0.1% Tween20) for 3x5min. Color reaction was carried out using BM purple as described above. For microscopic examination, slides were sealed and coverslipped using Permount (Fisher).

Table 2.1. Primers used in making *in situ* probes

Primer	Sequence
P1	Mouse Rasip1 *in situ* probe
	5-ÅATGCTATCTGGTGAACGAAAG-3 ô
	3-ÎTCAAGGTGTCGAAGCCACCG-3 ô
P2	*Xenopus tropicalis* Rasip1 *in situ* probe
	5-ÅTTAAGGGAAAGAGAAGAAAGCATCT-3 ô
	5-ÍCATACAGTGTCTTGGTCAGATAATATAC-3 ô
P3	VEGFR2 *in situ* probe
	5-ÍACGGAGAAGGAGTCTGTGC-3 ô
	5-ÍGGACAGGACCACTTCCAT-3 ô
P4	Primers to LacZ cassette
	5-ÍGTGGCGCTGGATGGTAAGC-3 ô
	5-ÍGCCATTTGACCACTACC-3 ô

ß-Galactosidase reaction

Embryos (or isolated organs) were fixed in 5mM EGTA (pH 8.0), 0.2% gluteraldehyde, 2mM $MgCl_2$ and PBS solution for 5 min on ice. After fixation, embryos were rinsed 3 times for 5 min in PBS. 50 mM Potassium Ferrocyanide ($K_4Fe(CN)_6ØH_2O$) and Potassium Ferricyanide ($K_3Fe(CN)_6$) solutions, stored at RT in dark, were used to make lacZ staining solution: 20 mM $K_4Fe(CN)_6ØH_2O$, 20 mM $K_3Fe(CN)_6$, 2 mM $MgCl_2$, 0.02% NP-40, add water or 1xPBS to 500 µl.

Staining solution was warmed to 37¯C before adding X-Gal (Growcells) to avoid X-Gal precipitation. 4 µl of 100 mg/ml X -Gal stock (in dimethyl formamide) was then added to the lacZ staining solution. Embryos were placed in staining solution and color reaction was allowed to develop at 37¯C overnight. When staining was evaluated to be optimal, embryos were washed with PBS 3 times for 5 min each, post-fixed in 4%PFA overnight, and transferred to 80% glycerol for viewing.

siRNA transfection

siRNAs obtained from Idt-DNA were transfected as per Idt-DNA's standard protocol. Briefly, for the 24-well format, 1.25µl of 20µM dicer substrate siRNA was diluted in 50µl of Opti -MEM I Reduced Serum Medium (Invitrogen) for each well. 1 µl of Lipofectamine 2000 (Invitrogen) transfection reagent was diluted in another 50µl of Opti -MEM I Reduced Serum Medium. After 5 minutes incubation at RT, the diluted siRNA and the transfection reagent were combined together, and incubated for 20 minutes at RT. MS1 cells (ATCC) were plated on a 24-well plate with a density of 5×10^4 cells/well in 400µl DMEM containing 10% FBS and without penicillin/streptomycin. The pre-mixed 100µl transfection complexes were then added drop-wise on top of the cells. After gentle mixing by rocking the plate back and forth, the cells were incubated at 37ęC in a 5% CO_2

incubator prior to following assays. siRNAs obtained from Invitrogen, and Dharmacon were transfected into cultured endothelial cells using standard protocol as previously described (Koh et al., 2008).

Endothelial cell assays

óTube formation assays were carried out in a 96-well plate. 50µl of Matrigel (BD Matrigel 354234) was thawed on ice and plated on the bottom of each well. ECs cultured in one well of a 24-well plate (90% confluency) were trypsinized, plated in one Matrigel coated well of a 96-well plate and cultured at 37ęC. When using wild type cells, the angi
starts to occur within a few hours. For better viewing, cells were stained with 1 M fluorescent dye Calcein-AM (Cell Biolabs) before microscopic examination. Quantification of angiogenic branchpoints was accomplished by counting observable branchpoints within 8 representative areas within each plated well.

óWound healing assays were carried out 7
Briefly, the cell monolayer is scratched using a sterile P200 pipet tip to create a ócell-freeô area (the wound). The cells were t
are then allowed to recover and imaging is

acquired immediately after scratching and rinsing, and also after an overnight incubation at 37ęC for comparison of wou
calculated as half of the total change in width.

Morpholino (MO) knockdown of Xenopus Rasip1

Xenopus tropicalis embryos were injected with 16ng *Rasip1*-MO (Gene-tools) into 1 cell at the 2-cell stage for assessment of vascular defects using *in situ* hybridization, or into both cells for assessment of transcript knockdown by RT-PCR. Embryos were allowed to develop to stage 32, then fixed in preparation for *in situ* hybridization. Morpholino-injected embryos were fixed in MEMFA (0.1M MOPS pH7.4, 2mM EGTA, 1mM $MgCl_2$, 4% PFA), transferred to 100% ethanol and stored at -20¯C. For evaluation of transcript knockdown efficiency, embryos were allowed to develop to either stage 25/26 or 29/30 and frozen directly on dry ice for RT-PCR.

Generation of Rasip1 null allele

The mouse 129sv genomic DNAs (provided by UTSW transgenic core) were used as template for the generation of a conditionally null allele by

amplifying a region of DNA flanking exon 3 and two additional homologous arms 5ô and 3ô using Takaraôs LA Taq polymerase into a neomycin/thymidine kinase double selection vector pGKneo-TK2-Floxed-Flip (kindly provided by Thomas Carroll). The exon 3 containing subclone was inserted into a multiple cloning site flanked by loxP sites. Neomycin resistance cassette was designed being flanked by Flp recombinase target (FRT) sites for removing if necessary. This targeting vector was electroporated into mouse embryonic stem cells by UTSW transgenic c Southern blot screening were PCR amplified and subcloned into pGEM-T-Easy vector (Invitrogen). SphI digested purified genomic DNA from each clones was screened by Southern blot using both probes for homologous recombination. The correct clone was injected into C57BL6/J blastocysts for generating Rasip1 targeted mouse line. After germ line transmission confirmation, the animals were bred with Sox2-Cre mice (kindly provided by Thomas Carroll) to generate a Rasip1 null allele. Litters were genotyped by PCR using primers listed in the Supplemental Experimental Procedures. The wild type, floxed, and null alleles give bands of 165 base pairs, 247 base pairs, and 331 base pairs, respectively.

Table 2.2. Primers for generating and genotyping Rasip1 null allele

Primer	Sequence
P5	5 ô homologous arm
	5-ôTCGGTACCCAGTTGGCATCGTGCTTCTA-3 ô
	3-ôGCGTCGACAGGGGATGTGTACTGCGTTC-3 ô
P6	3 ô homologous arm
	5-ôTCTTAATTAAGGCTTGCTCTTTCACAGGACCCTGG-3 ô
	5-ôTCTTAATTAATATGACAGCGGGACAGAGTGGGC-3 ô
P7	Rasip1 Exon3
	5-ôGTCCCTGCAGGCTCTCTGTTCACCTATTTCTTACCAAGG-3 ô
	5-ôGCTCCTGCAGGCCACGGCCACACAAACGACAAGAA-3 ô
P8	5 ô Southern blot probe
	5-ôGTCCAATACGCATAACCTGTTCT-3 ô
	5-ôGGCCATTTGACCACTACC-3 ô
P9	3 ô Souther blot probe
	5-ôCAGCTCTGCAATGACTTGGA-3 ô
	5-ôCAAAACCAAAACCCAACCTG-3 ô
P10	WT and floxed allele genotyping
	5-ôGGGGTGACAGTGGAACACA-3 ô
	5-ôCGGTGGGAAGAATGGAGATA-3 ô
P11	Null allele genotyping
	5-ôATGGTATGCCTGCCATTTGT-3 ô
	5-ôACGACTGTGCCTTCATGTTG-3 ô

Cell Culture

Human umbilical vein ECs (HUVEC, PCS100-010) and mouse pancreatic islet EC line MILE SVEN 1 (MS1, CRL-2279) were obtained from ATCC (or Lonza) and cultured per ATCC's standard 293AD cells (kindly provided by Eric Olson) were grown in Dul (DMEM, GIBCO) with 10% Fetal Bovine Serum (FBS).

Establishment of MS1$^{Rasip1\text{-}FLAG}$ cell line

C-terminal FLAG tagged Rasip1 cassette was inserted into pEN_TTmiRc2 and then sub-cloned into pSLIK-Neo (kindly provided by Zhijian Chen) by gateway cloning. 10µg Rasip1-FLAG expressing pSLIK vector was transfected into 293AD cells together with 7.5µg of each of the two packaging plasmids pLp1, and pLp2, and 5µg of the vesicular stomatitis virus (VSV) G envelope plasmid pLp-VSVG diluted in Opti-MEM (Invitrogen). The medium was changed 12 hours post-transfection, and the viral particles were harvested and filtered through 45 micron micro filters upon applying to MS1 ECs for infection. The infected MS1 cells were selected with 4mg/ml G418 (Sigma), and the expression of Rasip1-FLAG were analyzed by western blot and immunofluorescent staining using a monoclonal anti-M2 antibody (Sigma).

Tandem Affinity Purification of Rasip1 Complex

MS1$^{Rasip1\text{-}FLAG}$ cells were cultured with the presence of 1μg/ml doxycyclin for 3 days to induce the expression of exogenous Rasip1-FLAG fusion protein. The cell lysate from ten 10cm dishes were incubated with 50μl Anti -FLAG M2 Affinity Gel (Sigma A2220) as per Sigmaôs standard protocol. were eluted with 200μl 0.2mg/ml FLAG peptide (Sigma F3290). The elutes were then incubated with 5μg Rasip1 antibody (Abcam ab21018) or IgG agarose (Sigma A0919, for control) at 4C for 1 hour. The Rasip1 antibody bound protein complex were then incubated with 50μl rec -Protein G Sepharose 4B (Zymed 10-1241) at 4C for 1 hour, followed by elution with 40μl 0.1mg/ml human RASIP1 immunizing peptide (aa951-962, UTSW Peptide Synthesis Core Facility). The final elutes were resolved by SDS-PAGE and processed by silver staining using Invitrogenôs SilverQuest excised and subjected Spe to Mass Spectrometry as previously published (Xu et al., 2009b).

Immunofluorescent Staining

Cells cultured on glass coverslips were washed twice in PBS and fixed in 4% Paraformaldehyde (PFA) at RT for 10 min, followed by permeablization in PBSN (0.1% NP40 in PBS) at RT for 15 min. The cells were then blocked in

CAS-Block (Invitrogen) for 1 hour at 4C, followed by primary and secondary antibodies labeling in CAS-Block. The stained coverslips were mounted using VECTASHIELD HardSet Mounting Media with DAPI (Vector Labs H-1500) and examined by epi- or confocal fluorescence microscopy. For whole mount immunofluorescence, the mouse embryos were fixed in 4% PFA at 4C for 1 hour, and primary antibody staining was carried out at 4ºC overnight. For sectioned mouse embryo immunofluorescence, the tissues were processed as previously described (Villasenor et al., 2008). If necessary, antigen retrieval was done using Retriever 2100 in their Buffer B. The sections were then blocked in CAS-Block (Invitrogen) for 1 hour at 4C, followed by primary and secondary antibodies labeling in CAS-Block in a humid chamber. The mounting and imaging conditions are the same as described above.

EC lumen and tube formation in 3D collagen matrices

HUVECs were suspended as single cells within 3.75 mg/ml collagen type I matrices and allowed to undergo EC morphogenesis as previously described (Koh et al., 2008). Cultures were fixed at indicated time points with 3% glutaraldehyde for several hours. In some cases, cultures were stained with 0.1% Toludine Blue containing 30% methanol and de-stained with MilliQ H_2O, prior to

photography, visualization and analysis. Some 3D collagen gels were also extracted to examine protein expression or protein-protein interactions.

3D EC culture pull-down assays

EC Cultures were lysed at the indicated time-points using cold detergent lysis buffer and incubated with S protein agarose beads as described (Koh et al., 2008). In separate experiments, supernatants were incubated with GST-PAK-PBD or GST-RhoA-PBD protein beads (in the absence or presence of 100 nM GDP) for 90 min at 4ęC to assess the degre
The beads were washed four times with washing buffer. Bound active Cdc42/Rac1 or RhoA proteins were detected by Western blots.

Flow Cytometry

HUVECs detached from the dish by 50mM EDTA (pH8.0) treatment were washed with and resuspended as 10^7/ml in labeling buffer (Ca^{2+} free PBS containing 0.5% BSA). After incubation at 37C for 15 min with or without 5mM $MnCl_2$, the cells were labeled with primary antibodies at 1:50 for 30 min on ice. Cells were then washed twice and labeled with fluorophore conjugated secondary

antibody in labeling buffer at 4C for 30 min. After final wash (twice in chilled PBS), cells were resuspended in 500μl 1% PFA and subjected to FACS analysis (UTSW Flow Cytometry Facility).

Microscopy, Imaging and Statistical Analysis for in vitro Lumen Formation

Visualization and image acquisition of EC lumen formation was performed using an inverted microscope (CKX41: Olympus) and real time-lapse imaging of ECs undergoing lumen and tube formation was done using a Nikon TE2000-E system with a temperature-controlled chamber. Image analysis was performed using MetaMorph software. Statistical analysis of EC vasculogenesis was performed using SPSS 11.0 software. Statistical significances were assessed by a paired-samples *t test.*

CHAPTER III

Rasip1 is important for vascular morphogenesis

Most of the molecular mechanisms responsible for blood vessel formation are not yet well understood. For decades, much attention was given to the role of vascular endothelial growth factor (VEGF) and its influence on EC migration and proliferation (Ferrara et al., 2003; Yancopoulos et al., 2000). Recently, however, discovery of a host of endothelial óguidar

ECs and shape individual blood vessels, has broadened our understanding of how cell-cell signaling influences the morphogenesis of individual vessels and the vascular network as a whole. These signaling molecules include the Eph-ephrins (Kuijper et al., 2007), bone morphogenetic proteins (BMPs) (Lebrin et al., 2005; Moser and Patterson, 2005; Park et al., 2006), transforming growth factors (TGFbs) (Lebrin et al., 2005), Notch and Notch ligands (Roca and Adams, 2007) and many others. In addition, a number of cell-autonomous factors have also recently been shown to be critical for proper EC behavior and blood vessel formation. Many of these factors, such as small GTPases Ras, Rho, Rac, Cdc42, Pak and their many effectors/modulators (Fryer and Field, 2005; Garnaas et al., 2008; Gitler et al., 2003; Kranenburg et al., 2004; Merajver and Usmani, 2005;

Tan et al., 2008) are already known to drive basic cell processes such as cell migration, cell proliferation and establishment of cell polarity. Despite recent advances, the molecular mechanisms underlying much of blood vessel formation *in vivo* remain unclear, and elucidation of both extracellular signaling events and cell autonomous regulatory signaling cascades will advance our understanding of vascular specification and patterning, in both normal and pathological conditions (Coultas et al., 2005).

Many Ras family members and their regulators have been implicated in vascular development (Gitler et al., 2003; Henkemeyer et al., 1995; Tan et al., 2008), including EC migration (Sosnowski et al., 1993; Tan et al., 2008), capillary tube assembly (Connolly et al., 2002), angiogenesis (Aitsebaomo et al., 2004; Fryer and Field, 2005; Kranenburg et al., 2004; Merajver and Usmani, 2005), blood vessel homeostasis (Komatsu and Ruoslahti, 2005) and vascular permeability (Serban et al., 2008). Ras molecules are small GTPases widely shown to function as molecular switches coordinating multiple cellular behaviors like growth, proliferation, migration and differentiation. Ras GTPases cycle between the GTP-bound (active) and GDP-bound (inactive) states, under the influence of GAPs (**G**TPase **A**ctivating **P**roteins), and GEFs (**G**TPase **E**xchange **F**actors) (**Figure 3.1**).

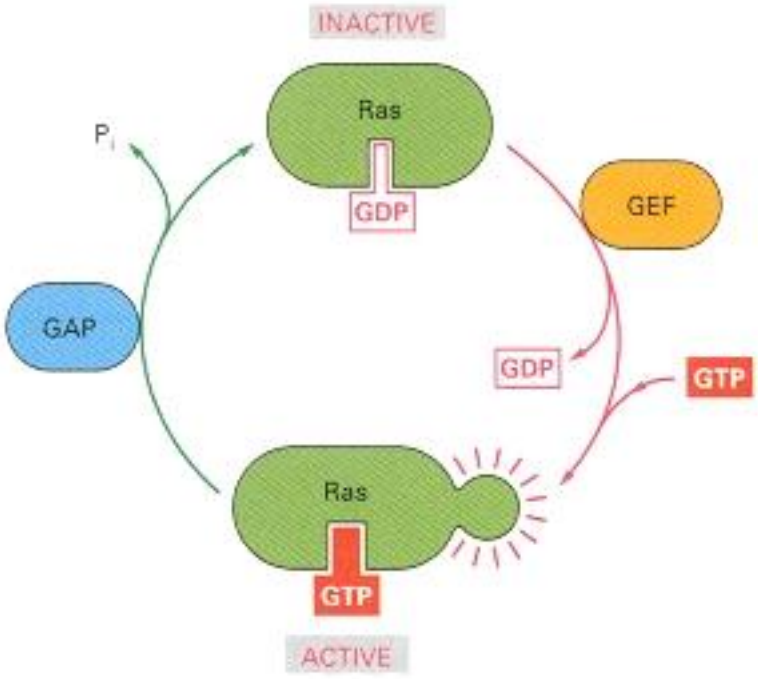

Figure 3.1. The regulation of Ras activity (Adapted from Figure 15-14, The Molecular Biology of the Cell., 4th edition. 2002) ñGTPase-activating proteins (GAPs) inactivate Ras by stimulating it to hydrolyze its bound GTP; the inactivated Ras remains tightly bound to GDP. Guanine nucleotide exchange factors (GEFs) activate Ras by stimulating it to give up its GDP; the concentration of GTP in the cytosol is 10 times greater than the concentration of GDP, and Ras rapidly binds GTP once GDP has been ejected é The Ras GAPs maintain most of the Ras protein (~95%) in unstimulated cells in an inactive GDP-bound state. ò

Ras family proteins have been shown to activate signaling cascades downstream of VEGF (Cross et al., 2003; Kranenburg et al., 2004; Roberts et al., 2004). VEGF stimulation of ECs increases the amount of activated Ras, while dominant negative Ras constructs inhibit VEGF-induced endothelial proliferation, migration and assembly (Meadows et al., 2001). However, although the Ras pathway proteins have been implicated in vascular development their exact role is not well understood.

Six years ago, Mitin and colleagues reported the identification of a novel Ras-interacting protein, Rasip1/Rain, which displays the characteristics of an endomembrane Ras effector (Mitin et al., 2004). Their experiments showed that Rasip1 possesses a Ras-associating domain (RA), homologous to the RA domains of other Ras effectors, and that Rasip1 preferentially binds to the GTP-loaded form of Ras, both *in vitro* and *in vivo*. Its enrichment in adult lung and high expression in transformed EC lines suggested the possibility that Rasip1 is expressed by ECs (Mitin et al., 2006).

In an effort to discover unknown regulators of blood vessel development, we performed a microarray screen that transcriptionally profiled embryonic aortal ECs (data not shown). Among numerous EC-enriched transcripts, we identified *Rasip1*. Here, we show that expression of *Rasip1* is strikingly restricted to the endothelium of the developing vasculature, in both frog and mouse, and we

demonstrate that *Rasip1* is essential for proper endothelial cell angiogenic assembly and migration, both *in vivo* and *in vitro*. We propose that *Rasip1* plays important roles during vasculogenesis and angiogenesis, possibly regulating the function of Ras proteins in ECs.

Identification of Rasip1 expression in murine endothelial cells

To identify sequences enriched in the embryonic dorsal aortae, we carried out Affymetrix microarray screening of aortal ECs from E8.25 mouse embryos (data not shown). dChip (Li and Wong, 2001) and Genespring software analysis was used to compare array data (to non-vascular array sets) and extract endothelial-enriched sequences. We initially identified *Rasip1* as an EST (AI853551) showing 50-fold enrichment in ECs over other tissues. A longer clone was acquired commercially (OpenBiosystems), allowing production of Dig-labeled antisense probes encompassing the region from exon 4 through exon 12 (~2000bp) of the *Rasip1* transcript. The *Rasip1* genomic structure has been previously described (Mitin et al., 2004), however no developmental expression or function has been reported.

Rasip1 is expressed in vascular endothelium during vascular plexus formation (E7.5-E10.0)

Using *in situ* hybridization, we characterized embryonic expression of *Rasip1* in mouse embryos and found it to be principally expressed in vascular endothelium. At E7.0 *Rasip1* is initially detected in the parietal yolk sac, in a punctate ring of cells (data not shown). Soon thereafter, at E7.5, expression expands to scattered cells of the extraembryonic yolk sac blood islands (**Figure 3.2A**). At E8.0, individual cells expressing *Rasip1* within the extraembryonic mesoderm can be observed at increasingly ventrolateral locations, in regions previously described as containing angioblasts (Drake et al., 2000; Ferkowicz and Yoder, 2005). The punctate appearance of *Rasip1* expression in extraembryonic tissues at this stage suggests that these cells are angioblasts (**Figure 3.2B**), as it closely resembles that of vascular endothelial growth factor receptor 2, *VEGFR2* (or *Flk1/KDR*), and Tal1 both established markers for early angioblasts (Drake and Fleming, 2000). At E8.25-E8.5, *Rasip1* is strongly expressed throughout the embryonic and extraembryonic endothelium in a pattern recognizable as the primary vascular plexus, including the endocardium, the forming dorsal aortae and the primordia of the cardinal veins (**Figure 3.2C,D**). During these stages, vasculogenesis of the principal embryonic blood vessels is occurring and major

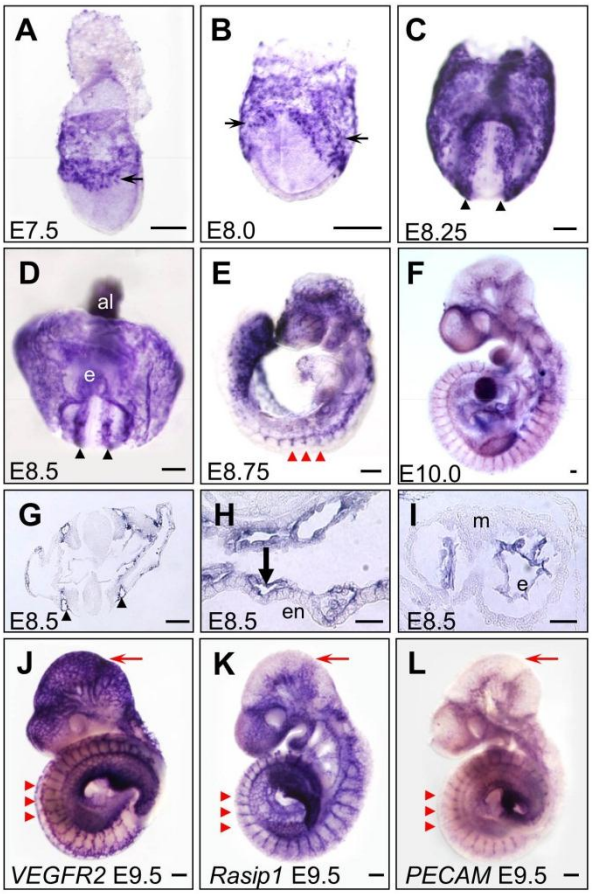

Figure 3.2. Expression of *Rasip1* in vascular endothelium during early embryogenesis. (**A-F**) Whole mount *in situ* hybridization showing whole stained embryos. Note expression in both scattered angioblasts (thin arrows), forming dorsal aortae (black arrowheads), intersomitic vessels (ISVs) (red arrowheads) and yolk sac vessels (thick arrows). (**G-I**) Transverse sections of *in situ* hybridizations showing endothelial-specific expression of *Rasip1* in (**G**) dorsal aortae, (**H**) yolk sac vessels, and (**I**) heart endocardium. (**J-L**) Comparison of *Rasip1* expression with that of the vascular markers *VEGFR2* and *PECAM*, in E9.5 embryos. Note overall similarity of expression, especially in the ISVs (red arrowheads) and trunk vessels. Note difference in intensity of vascular staining in distinct regions, such as the cephalic vessels (red arrows). al, allantois; e, endocardium; en, endoderm; m, myocardium. The scale bars represent 200μm in all panels except J-L, where they represent 50μm.

vessels are taking shape (i.e. parallel dorsal aortae in **Figure 3.2D**) (Walls et al., 2008).

As embryogenesis continues, *Rasip1* expression continues to be expressed in developing blood vessels. After embryonic turning, at E8.75, expression is evident in all large and small blood vessels, including the sprouting intersomitic/intersegmental vessels (ISVs) (**Figure 3.2E**). Expression of *Rasip1* within ISVs of later embryos (**Figure 3.2E,F**) suggests a role not only during vasculogenesis, but also during extension of vascular sprouts, or angiogenesis. Transverse sections through E8.5 embryonic tissues reveal that expression is restricted to the endothelium in all tissues examined, including the dorsal aortae (**Figure 3.2G**) and yolk sac vessels (**Figure 3.2H**). In addition, *Rasip1* is expressed within the endothelium of the endocardium, but not in myocardium (**Figure 3.2I**).

We compared expression of *Rasip1* with that of other known vascular markers, such as *VEGFR2* and *PECAM* (**Figure 3.2J-L**), and found that *Rasip1* outlined almost identical vascular structures in the developing embryo. For instance, expression of all three markers was observed in aortae, ISVs, endocardium and vessels of the lateral plate and head mesoderm. Of note, different vascular beds appeared to express these three vascular markers with varying intensity. For instance, the head plexus of E9.5 embryos expressed

VEGFR2 more robustly, while *Rasip1* was more strongly expressed than either *VEGFR2* or *PECAM* in the ISVs and endocardium (**Figure 3.2J-L**). These differences reveal surprising endothelial heterogeneity at early stages of vascular development. Nonetheless, overall expression analysis suggests that *Rasip1* is primarily restricted to vascular endothelium.

Rasip1 during late embryogenesis (E10.5-birth)

Analysis of *Rasip1* transcripts later during development reveals their expression in established vessels. Expression could indeed be detected in the blood vessels of various organs throughout midgestion stages (**Figure 3.3**). Specifically, we found *Rasip1* strongly expressed in the vessels of all embryonic organs and tissues examined, including heart, lung, head, limb bud, pancreas, spleen and stomach (Xu et al., 2009a). When compared to the expression of *VEGFR2* and *PECAM*, we found that *Rasip1* generally marked identical vascular beds, with only slight variations in expression intensity. Expression of *Rasip1* in later embryonic vessels, after their formation via either vasculogenesis or angiogenesis, implies that it has a maintenance function in mature vessels. Indeed, *Rasip1* continued to be expressed in the endothelium of vessels into postnatal stages (Xu et al., 2009a) and was detected in adult organs, particularly in the highly vascularized lung (Mitin et al., 2004).

Figure 3.3. Vascular expression of *Rasip1* in embryonic organs and tissues. A, D columns) Whole mount β-galactosidase staining using *Flk1*(*VEGFR2*)-lacZ embryos. Whole mount *in situ* hybridization of *Rasip1* (**B, E** columns) and *PECAM* (**C, F** columns). (**A-F**) Hearts. (**A-C**) Lungs. (**A-C**) Heads. (**D-F**) Limb buds. Note similarity of expression of *Rasip1* in most vessels, as marked by *VEGFR2* and *PECAM* expression (black arrowheads). Expression of all three vascular markers can be observed in the endocardium of the ventricle trabeculae in the heart (A-C) and of the coronary vasculature (arrows, D-F). Expression of all three markers is evident in the proximal ECs of the aPECAM is not expressed in the ECs of (A) the most distal tips of the buds at E10.5 (red arrowheads), while both *VEGFR2* and *Rasip1* are observed in this population. This heterogeneity is also observed in the cephalic vessels at E10.5, where *VEGFR2* is robustly expressed in the most mediolateral/distal vessels of the mesencephalon, while *Rasip1* and *PECAM* are expressed at low (white arrows) levels (Rasip1 is expressed in the vessels of the developing limb buds, including the interdigit vessels (white arrows), Da, dorsal aorta; b, bronchus; br, branchial ventricle. The scale bars represent 100μm in A-F and in 25μm.